

IET ***Nanobiotechnology***

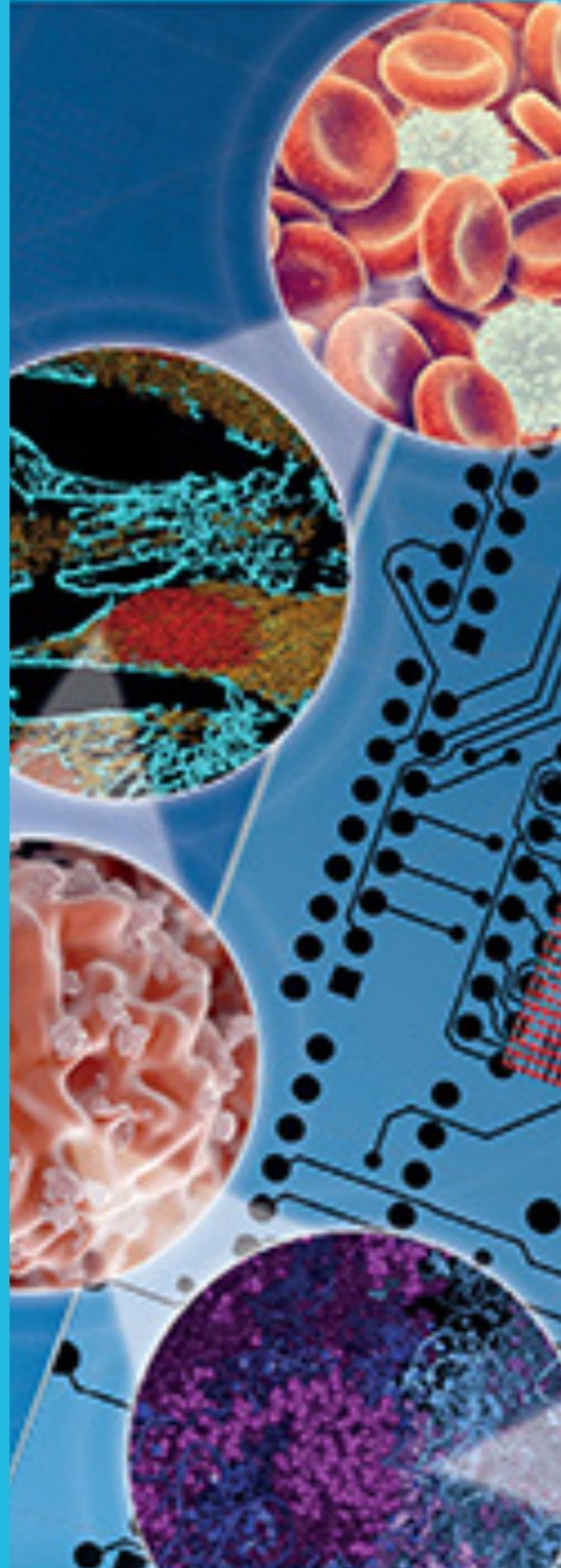
Special issue **Call for Papers**

**Be Seen. Be Cited.
Submit your work to a new
IET special issue**

**"Micromechanics in Biology
and Medicine"**


**Guest Editors: David
MacManus, Majid
Akbarzadeh Khorshidi,
Mazdak Ghajari and Hamid
M. Sedighi**

Read more



ORIGINAL RESEARCH

Enhancement of antibacterial activity through phyto-fabrication of silver nanoparticles with *Ficus thonningii* aqueous extracts

Dickens A. Ondigo^{1,2} | Were L. L. Munyendo¹  | Dickson Andala² |
Apollo O. Maima³ | Josephat M. Mosweta¹ | Kevin W. Odhiambo¹

¹School of Pharmacy & Health Sciences, United States International University—Africa, Nairobi, Kenya

²Faculty of Science & Technology, Multimedia University, Nairobi, Kenya

³School of Pharmacy, Maseno University, Maseno, Kenya

Correspondence

Dickens A. Ondigo and Were L. L. Munyendo, School of Pharmacy & Health Sciences, United States International University—Africa, P.O. Box 14634 -00800, Nairobi, Kenya.

Email: dondigo@usiu.ac.ke and lmunyendo@usiu.ac.ke

Abstract

The World Health Organisation reports higher levels of bacterial resistance to cephalosporins and carbapenems of above 54%. The sufficient redox capabilities of *Ficus thonningii* phytochemicals for Ag⁺ reduction to Ag⁰ and ultimately aggregation to nucleation are exploited for the first time in attempting to enhance the antibacterial activity. Solution colour change to brown due to surface plasmon resonance phenomenon confirmed nanoparticle fabrication with a UV/Vis absorption peak at 426 nm. Fourier Transform Infrared spectra revealed functional groups (C=C at 1620–1680 cm⁻¹; C=H at 1400–1600 cm⁻¹ aromatics) for encapsulation, stabilisation, and reduction of the silver ion. The Dynamic Light Scattering technique verified *F. thonningii* encapsulated silver nanoparticles particle size of 57.84 nm with a negative zeta potential (−19.8 mV) as proof of stability. The surface, shape and topographical features were shown by Scanning Electron Microscopy as spherical orientations. An enhanced antimicrobial efficacy was displayed by the nanoparticles (inhibition zones of 26.1, 24.1 and 15.2 mm from 11.5, 10.6 and 6.5 mm) for *Staphylococcus aureus*, *Streptococcus pyrogenes* and *Escherichia coli*, respectively, compared to Flucloxacillin standard that was in the ranges of 21.5, 23.5 and 25.7 mm. The enhanced potency provides a basis for diversified approaches of generating novel drugs for treating bacterial infections.

1 | INTRODUCTION

The use of antibiotics in the management of infectious diseases has been effective over the years. However, repeated use of conventional anti-infective drugs has led to the development of antimicrobial-resistant strains [1]. The antimicrobial resistance (AMR) to the antibiotic regimen is a major problem to Africa and world over, and the failure to control it is resulting in increased mortality, worsening clinical conditions and rise in treatment costs due to prolonged hospital stays.

Nanotechnology continues to gain much traction as a truly emerging and proven inter-disciplinary science with numerous areas of application. This is due to nanoparticles' extraordinary physico-chemical properties applied in various

fields, including health care, clean energy, engineering and electronics [2]. Recently, several research studies have reported results of successful synthesis of Au and Ag nanoparticles by green syntheses using various biological extracts from different plant species. Green synthesis is pretty ideal for generation of nanoparticles by phytocompounds. Some of its positive attributes include simplicity of the processes, ready scalability and cost-effectiveness. Furthermore, the phytocompounds are non-toxic and act both as reducing and stabilising agents in the syntheses of nanoparticles [3]. Stabilisation of phytochemicals is of great importance in achieving the therapeutic efficacy by prolonging residual time at a site of action. Synthesis and screening of antimicrobial activities using the fabricated AgNP's were interrogated utilising *Cleome viscosa* extracts [4]. Most recently, essential oils

This is an open access article under the terms of the Creative Commons Attribution-NonCommercial License, which permits use, distribution and reproduction in any medium, provided the original work is properly cited and is not used for commercial purposes.

© 2022 The Authors. *IET Nanobiotechnology* published by John Wiley & Sons Ltd on behalf of The Institution of Engineering and Technology.

of *Ferula persica* (common name: wild gum) were used to fabricate gold nanoparticles [5, 6] and in both cases, valuable results were obtained.

The *Ficus thonningii* species has a composite of phytochemicals that are useful as capping, reducing and stabilising agents in the synthesis of nanoparticles, such as tannins, saponins and flavonoids, which also exhibit healing properties, and hence their medicinal values [7]. Silver nanoparticles (NPs) have gained and drawn attention due to their extensive applications in areas, such as integrated circuits, sensors, biolabelling, filters, and antimicrobials capabilities. Consequently, these properties have influenced the use of these NPs in different fields of medicine, various industries, animal husbandry, packaging, accessories, cosmetics, health and military [8, 9].

In this research, *F. thonningii* stem bark extracts were used in the synthesis of AgNP's due to their active antimicrobial properties [10, 11]. The presence of medicinally active secondary metabolites in the plant [12] thus presents it as a good candidate for biogenic synthesis of silver nanoparticles. This project exploited a modern, benign and cost-effective approach in applying nano-technological advances to enhance the potentials of plant products as antibiotics for the prevailing drug resistance.

2 | RESULTS

2.1 | Extraction yields

The percentage yields in the extraction processes were calculated and tabulated in Table 1.

2.2 | Phytochemical screening

The water extracts displayed the highest percentage yield significantly above the ethyl acetate and ethanol and the phytochemical profile evaluation was thus carried out only for the water extract. An array of groups of phytochemical compounds was appropriately tabulated in Table 2.

TABLE 1 Percentage yield of *F. thonningii* extracts

Plant part	Extraction solvent	Plant powder weight (grams)	Extract weight (grams)	Percentage yield (%)
Stem bark	Water	100	4.5	4.5
	Ethanol	100	1.5	1.5
	Ethyl acetate	100	0.75	0.75
Leaves	Water	100	1.5	1.5
	Ethanol	100	2.0	2.0
	Ethyl acetate	100	0.5	0.5
Root bark	Water	100	1.2	1.2
	Ethanol	100	2.7	2.7
	Ethyl acetate	100	1.15	1.15

2.3 | Optimization of *F. thonningii* nanoparticles synthesis by taguchi orthogonal array

Design-Expert[®] version 12.0.0 was used for generation and evaluation of the Taguchi experimental design. The design involving four factors at three levels entailed an array of 9 rows and four columns (Table 3). The mean of triplicate results for each of the nine experiments was taken. The responses for optimality were taken as absorbances and zones of inhibition (in mm). The optimum variables for green synthesis of *F. thonningii* encapsulated nanoparticles were stem bark, water extract at a volume of 5 mL and stirring time of 12 h.

2.4 | Characterization of *F. thonningii* nanoparticles

2.4.1 | UV/ spectroscopy

The formation of *F. thonningii* Silver Nanoparticles (*Ft*-AgNP's) was observed at 426 nm with peak absorbances

TABLE 2 Phytochemical constituents of leaves, stem bark and roots of *F. thonningii*

Phytochemicals compounds	Inference for parts		
	Leaves	Stembark	Roots
Alkaloids	+	++	-
Antraquinones	-	+++	-
Flavonoids	+	+++	-
Tannins	+	++	+
Simple phenolic compounds	+	++	+
Saponins	+	+++	+
Terpenoids	+	+	-
Reducing sugars	+	+	+

Abbreviation: -, phytochemicals not detected; +, phytochemicals detected; ++, phytochemicals detected in minimal amounts; +++, phytochemicals detected in quite high amounts.

varying in line with the stirring time. The UV/Visible absorption spectra of the AgNPs showed maxima peaks - between 425 and 430 nm with red or blue shifts as a confirmation of nanoparticle generations (Figure 1a). This was verified by the absence of peaks at a wavelength above 400 nm for the *F. thonningii* crude extract (Figure 1b).

2.4.2 | Fourier-Transform Infra-Red Spectroscopy

The FTIR spectroscopy analysis of the green synthesis starting materials and generated nanoparticles provided handy information on functional group transformations as indicated in Figure 2.

2.4.3 | Zeta size and zeta potential analysis

The analysis of the prepared AgNP's colloidal system showed that the isolated particles exhibited an average hydrodynamic diameter of 57.84 nm in deionised water. The electrophoretic

mobility distribution of the AgNP's had a mean of 0.4873 $\mu\text{mcm}/\text{vs}$ and a ζ -potential measurement of -19.8 ± 0.2 mV at a temperature of 25.0°C with an minimal Polydispersity index of 0.329 (Table 4).

2.4.4 | Scanning Electron Microscopy

The SEM images of the *Ft*-AgNP's as shown in Figure 3 showed shiny spherical and oval particles with sizes ranging from 50 to 100 nm.

Elemental mapping of *F. thonningii* AgNP's showed the presence of Ag^+ as nanoparticles indicated by higher counts at 3 keV in Figure 4.

2.5 | Antibacterial assays

The antimicrobial properties of the crude *F. thonningii* extracts and the *Ft*-AgNP's were assayed against *Staphylococcus aureus*, *Streptococcus pyogenes* and *Escherichia coli* bacterial strains and zones of inhibition recorded as in Table 5.

Plant part	Extraction solvent	Extract volume	Stirring time	Absorbance	Zones of inhibition
Leaves	Water	1.0	2.0	0.3815	13
Stem bark	Ethanol	1.0	0.5	0.1642	0
Root bark	Ethanol	5.0	2.0	1.0362	23
Root bark	Ethyl acetate	1.0	12.0	0.6097	21.5
Stem bark	Water	5.0	12.0	1.7613	23.8
Stem bark	Ethyl acetate	2.5	2.0	0.5681	19
Leaves	Ethyl acetate	5.0	0.5	0.4061	18
Root bark	Water	2.5	0.5	0.1866	12
Leaves	Ethanol	2.5	12.0	1.1644	22.5

TABLE 3 Orthogonal array

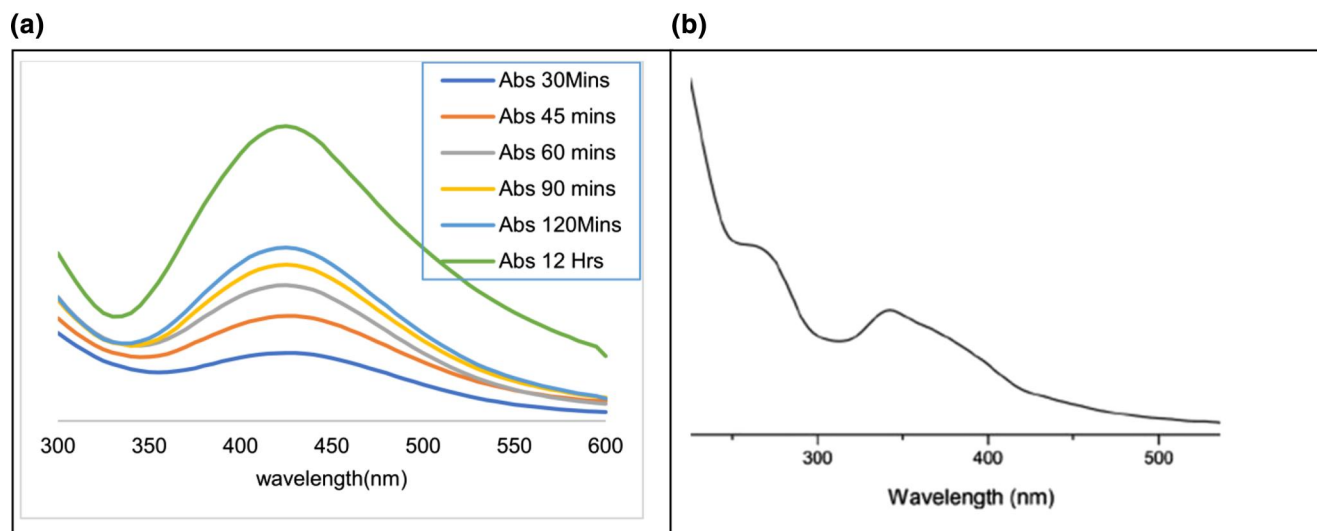


FIGURE 1 (a): *F. thonningii* AgNP's Ultra violet/visible (UV/Vis) absorption for various stirring time values [30, 45, 60, 90, 120 min and 12 h]. (b): *F. thonningii* crude extract UV/Vis - absence of peaks at a wavelength above 400 nm

2.6 | Statistical analysis

The analysis of variance (ANOVA) was performed using the Statistical Product and Service Solutions (SPSS) and results tabulated in Table 6 accordingly for sum of squares, degrees of freedom, and mean squares. The various factors' contribution was also calculated and appropriately recorded.

Based on absorbance as the response factor, the highest percent contribution was from the extract amount (32.2%). This confirmed the silver nitrate reduction capability in the formation of nanoparticles. The reduction potential is thus realized to be directly proportional to the extract amount (reducing agent). Regarding the zone of inhibition as a response, the length of stirring time displayed the highest percent contribution to the generation of nanoparticles with the enhanced bioactivity.

3 | DISCUSSIONS

The stem bark yielded the highest amount of extracts as compared to the other parts of the plant. This could be attributed to the thickness of the stem bark that was observed to contain significant amounts of crude fibre. Its exudates in the form of latex has also been harnessed for ethnobotanical application [10].

Phytochemical screening of the crude extracts of leaves, stem bark and roots of *F. thonningii* indicated the presence of alkaloids, carbohydrates, flavonoids, saponins and tannins at

different levels of concentration. Flavonoids and anthraquinones were not found in the leaves and root extracts though the same were abundant in the stem bark. The stem bark was thus chosen as the main source of the phytochemicals to be applied in green synthesis of nanoparticles. Significantly, *F. thonningii* flavonoids have been reported to exhibit the antibacterial activity through the formation of complexes with extracellular and soluble proteins [7].

Successful fabrication of nanoparticles by green synthesis is dependent on several variables requiring optimization to assure stable nanoparticles with the desired residence time during therapeutic applications. In the phytochemical evaluation of *F. thonningii* extract, flavonoids were abundantly present, and FTIR spectra revealed functional groups (O-H, N-O, C=C, N-H) known to participate in redox

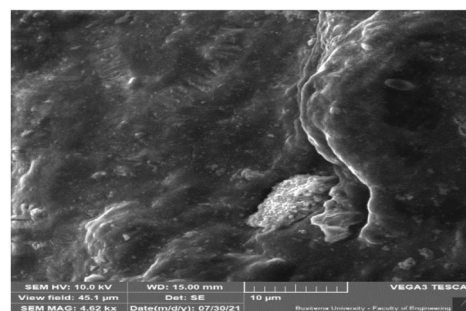


FIGURE 3 Scanning Electron Microscopy (SEM) image of *Ft-Ag* NPs

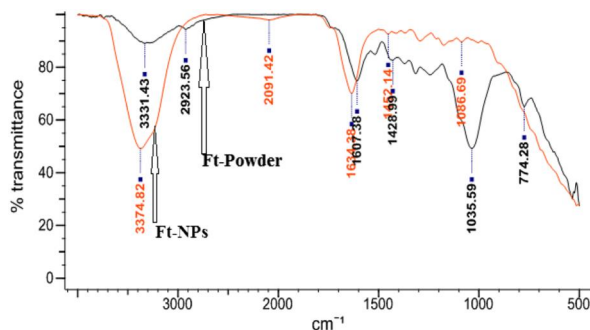


FIGURE 2 Fourier-Transform Infra-Red (FTIR) spectra for encapsulated *Ft-AgNP*'s and plant extract

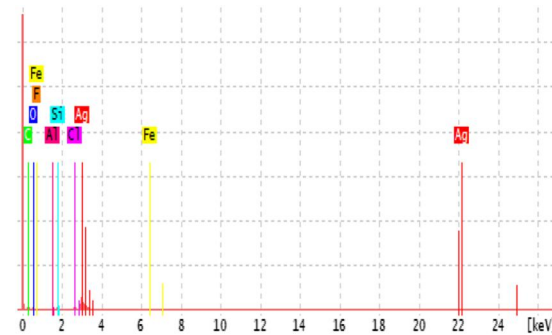


FIGURE 4 The EDX peaks of *Ft-Ag* NPs

TABLE 4 Particle size analysis, Zeta potential and polydispersity index

Particle size analysis			
<i>Ft-AgNP</i> 's	Zeta sizes (nm)	Average size (nm)	Polydispersity index
	63.96 - 47.65	57.84	0.329
Zeta potential			
<i>Ft-AgNP</i> 's	Zeta potential (mv)	Zeta deviation	Conductivity (ms/cm)
	-19.8	6.22	0.266
Electrophoretic mobility			
<i>Ft-AgNP</i> 's	Mobility	Deviation	Conductivity
	-1.550	0.4873	0.266

TABLE 5 Zones of inhibition in mm

Test solution	Concentration (µg/ml)	Zones of inhibition (mm)		
		<i>Staphylococcus aureus</i>	<i>Streptococcus pyogenes</i>	<i>Escherichia coli</i>
Crude extract	10	21.6	22.7	7.8
	1	11.5	10.6	6.5
	0.1	9.3	6.0	6.0
	0.01	6.0	6.0	6.0
<i>Ft</i> -Ag-NPs (10 µg/ml)	10	27.5	25.2	22.8
	1	21.5	19.8	15.2
	0.1	24.1	19.8	14.8
	0.01	10.3	8.0	6.0
Flucloxacillin std (1 µg disc)	1	25.7	23.5	21.5
Control: Distilled water	0	NIL	NIL	NIL

TABLE 6 ANOVA analysis of factors for percent contribution

FACTOR	SS ^a	DF ^b	MS ^c	PC(%) ^d
Absorbance				
A-plant part	0.0827	2	0.0414	3.7
B-solvent extraction	0.1296	2	0.0648	5.8
C-extract amount	0.7143	2	0.3571	32.2
D-stirring time	1.29	2	0.6462	3.7
Pure error	0	0		
Cor total	2.22	8		
Zones of inhibition				
A-plant part	34.58	2	17.29	7.4
B-solvent extraction	30.44	2	15.22	6.5
C-extract amount	156.31	2	78.15	33.4
D-stirring time	246.41	2	123.2	52.7
Pure error	0	0		
Cor total	467.74	8		

^aSum of squares.^bDegrees of freedom.^cMean squares.^dPercent contribution.

reactions. In the nanoparticle synthesis, therefore, plausibly Ag^+ ion is reduced to Ag^0 by mainly ‘-OH’ and ‘=O’ functional groups of saponins, anthraquinones and flavonoids as contributors of extract's sufficient reduction potential [13]. The zero-valent iron particles get oxidised under basic conditions and ultimately aggregate. This is followed by nucleation that results in the formation of Ag_2O_3 nanoparticles capped by the phytochemicals as reported by Vinayagam group in 2021 [14].

Design Expert software enabled systematic optimization of variables. In the biogenic reduction of Ag^+ ion to Ag^0 [15], stirring time interval played a key role in the synthesis of the nanoparticles at an ambient temperature. This was easily noted

via the colour change of the reactants from a pale yellow to a dark brownish shade. Confirmation from a UV/Vis maximum absorption at 426 nm by the *Ft*-AgNP's illustrated Surface Plasmon Resonance (SPR), a phenomenon involved in the reduction of metal ions [16]. This colloidal silver NPs' pale yellow to dark brown colour is explained by resonance from SPR phenomenon features, which also depends on the size, shape, and concentration of the NPs [17]. Similar results were noted by Mohammadlou et al. in 2016 [18] and Gogoi group in 2015 [19] both of who applied the green synthesis technique in the fabrication of Ag nanoparticles.

The FTIR spectra of *F. thonningii* plant extract showed peaks at 3331, 2924, 1607, 1516, 1452 and 1036 cm^{-1} . This indicated the presence of functional groups as N-H/O-H (about 3300 cm^{-1}), C-H (2850–3000 cm^{-1}), C=C (1620–1680 cm^{-1}), N-O (1515–1560 and 1315–1369 cm^{-1}), C=H (1400–1600 cm^{-1} aromatics) and C-O (1000–1150 cm^{-1}) [20]. Meanwhile, encapsulated silver nanoparticles (*Ft*-AgNP's) showed peaks at 3376, 2085 and 1633 cm^{-1} , which give credence to the presence of the functional groups O-H/N-H (around 3300 cm^{-1}), $\text{C}\equiv\text{C}$ (around 2100 cm^{-1}) and C=C/C=O (around 1620 cm^{-1}) vibration stretch. The strong absorption band at 3376 cm^{-1} indicates the presence of O-H stretch (H-bonded) of alcohols or phenols. The O-H stretching vibration of the carboxylic acids and C-H stretching of alkenes appears as a peak at 2924 cm^{-1} . The O-H and N-H functional groups could be perceived to be responsible for the strong reducing functionalities based on variations in peak positions. Capping of the nanoparticle comes from the absorption band at 1036 cm^{-1} from C-O stretch of alcohols, carboxylic acids, esters, ethers and C-N stretch of aliphatic amines [21].

Dynamic Light Scattering enabled determination of particle size, surface charge as zeta potential and Polydispersity Index (PDI). These results demonstrate coherent stable nanoparticles similar to the findings of Amereh et al., 2019 [22]. The size of the *Ft*-AgNPs formed averaged 57.84 nm with a negative surface charge. As a rule of thumb, absolute Zeta Potential (ZP) values above ± 30 mV indicate higher stability [23]. In this case, ZP values of -20 mV obtained revealed a

responsive stabilisation. Scanning Electron Microscopy images of the *Ft*-AgNP's showed shiny spherical and oval particles of average sizes ranging from 50 to 100 nm. Though there were some notable aggregation, isolated individual particles were also identified, confirming the zeta sizing results. Moreover, EDX elemental mapping revealed the presence of Ag at 50.4%, C at 22.3% and 19.8% for oxides by a strong EDX peak at around 3 keV, which is a typical absorption for metallic silver nanoparticles. Additionally, high proportions of other elements, such as Al, Fe and O, were evident. The O peaks are from the biomolecules bound to the surface of the silver nanoparticles, and Al and Fe peaks are due to a sample grid holder, which is made from the alloy. Meanwhile, the nanoparticles having been synthesised by plant materials, F, O, C, Si, and Cl peaks manifested as signals of capping organic materials from the plant tissue microelements involved in usual physiologic functions [3].

In the Kirby-Bauer agar well method for antibacterial activity evaluation, the results obtained showed that encapsulated *Ft*-AgNPs displayed more increased inhibitory activities against gram-positive *S. aureus* and *S. pyogenes* agents as compared to gram-negative *E. coli* relative to the flucloxacillin standard drug concentration. These results are similar and in agreement with earlier findings [19, 24]. This notable increase in antimicrobial efficacy with the nanoparticles of 26.1, 24.1 and 15.2 mm from 11.5, 10.6 and 6.5 mm, by the crude extract for *S. aureus*, *S. pyogenes* and *E. coli*, respectively, could be attributed to the presence of active phytochemical compounds encapsulated to silver nanoparticles, thereby increasing surface area and sustained residence time [25]. The finer particle sizes and increased surface area of the synthesised nanoparticles significantly contributed to the enhanced antimicrobial efficacy. The AgNPs have been reported to facilitate the production of reactive oxygen species [26], which are able to cause damage to the DNA and the bacterial protein, leading to the bactericidal activity against the bacterial cell strain [27]. This bactericidal effect maybe further attributed to the shape and size of the *Ft*-AgNP's. The smaller size easily penetrates the cell membrane of the bacterial walls, hence causing lysis of the same [28]. The antibacterial activity is witnessed to increase to equal magnitude for both gram-positive and gram-negative bacterial strains. This study presents for the first time an illustration that green-synthesised nanoparticles' antibacterial activity results from Ag⁺ ion interaction with thiol groups of *E. coli* (Gram negative) cell wall protein. Meanwhile, the reactive oxygen species from phytochemical functional groups lead to the damage of the DNA of gram-positive bacterial strains [29].

4 | CONCLUSION

A benign green and ecofriendly approach for the synthesis of encapsulated silver nanoparticles using the *F. thonningii* stem bark plant extract enabled fabrication of the *Ft*-AgNP's. The formed nanoparticles were spherical in shape with a particle distribution range of 47–63 nm. The synthesised *Ft*-AgNP's enhanced the antibacterial inhibitory range against both the

gram-positive and gram-negative strains. The green synthesis approach for AgNPs especially with known medicinal plant extracts for antibacterial purposes against pathogenic human strains opens a new path in the antibacterial drug discovery.

5 | EXPERIMENTAL

5.1 | Materials, reagents, cultures and instruments

F. thonningii is a multi-stemmed, evergreen or briefly deciduous tree with a dense, rounded to spreading crown, which belongs to the Moraceae family. It is commonly found well distributed in upland forests, open grasslands, riverine and rocky areas [9]. It grows well on a variety of soils but prefer light, dried and well-drained soils with neutral reaction to acid. It is also found in the savannahs. Normally, it is propagated by cutting and seed dispersal by birds and animals.

Solvents as hexane, dichloromethane, acetone and methanol were all GPR grade and hence distilled before use for extraction. All the other chemicals utilised for biochemical assays were of Analytical Grade and hence used as obtained without further processing. The chemicals were all sourced from Sigma Aldrich Company through their local agents Kobian Laboratory supplies of Nairobi, Kenya.

The instruments used included a Carry 60 UV/VIS Spectrophotometer by Agilent (USA); JASCO 4700 ATR- FT/IR (Japan); REMI Microcentrifuge, RM-12C (China); Vega 3 TESCAN Scanning Electron Microscope (Czech Republic); Malvern Zeta-sizer Nano series (Worcestershire, U.K); and Willey Mill (India).

S. aureus (ATCC 25922), *S. pyogenes* (ATCC 27853) and *E. coli* (ATCC 25921) were acquired from Laboquip Laboratory supplies, Nairobi Kenya.

5.2 | Plant collection and processing

The plant samples of *F. thonningii* (common wild fig or strangler fig) were identified, authenticated and collected with the aid of a taxonomist at Esageri, Eldama Ravine, Baringo County. Voucher Specimen (No. ONDIGO O-010) has been retained at the USIU-Africa Herbarium. The stem bark, leaves and root samples were cut using a sterile knife and transported back to School of Pharmacy and Health Sciences of USIU-Africa in polythene bags. The collected plant samples were cleaned using distilled water and then air dried at room temperature for a period of 14 days. The dry samples were ground into fine powder using the Willey mill and stored in airtight containers awaiting further experimental procedures.

5.3 | Solvent extraction

Some 100 g each of powdered *F. thonningii* leaves, stem bark and root were accurately weighed out into 1000 ml Erlenmeyer

flasks and macerated for 48 h using distilled water at room temperature. The prepared plant extracts were then filtered through a Whatman filter paper No 1 and supernatant solutions kept in clean vials. The same procedure was repeated but now utilising ethanol as the solvent.

5.4 | Phytochemical screening of *F. thonningii* plant extracts

The phytochemical profiling of aqueous extracts was done according to Prod et al., 2012 [13]. To detect flavonoids, 1 ml of concentrated H₂SO₄ was added to 5 ml of water extract and 0.5 g of Magnesium strip. A pink or red colouration that disappeared on standing for 3 min indicated the presence of flavonoids. Test for tannins was by taking 2 ml of the aqueous extract and adding it to 2 ml of water; after which 2 drops of diluted ferric chloride solution was added. A dark green or blue green colouration indicated the presence of tannins. The presence of saponins was determined by taking 1 ml of aqueous extract, then 2 mL of distilled water added in a test tube before solution being shaken vigorously and observed for 20 min for a stable persistent froth. Alkaloids were detected by 20 ml of water extract being evaporated and dry residue, then dissolved in 5 ml of HCl (2N) and filtered. The positive alkaloid test was revealed by the presence of precipitate upon addition of Mayer's reagent. Carbohydrates as reducing sugars were tested by adding 10 drops of boiling Fehling's solution to 2 ml water extract in tubes. Formation of a brick-red precipitate in the bottom of the tube indicated the presence of reducing sugars. The aqueous extract (5 ml) was treated with iodine reagent to test for presence of starch. A shift to blue violet indicated the presence of starch. The presence of anthraquinones was determined by adding 10 ml of benzene to 6.0 g of the *F. thonningii* powder sample in a conical flask and then soaking for 10 min before filtration. To the filtrate, a 10 ml of 10% ammonia solution was added and shaken vigorously for 45 s. A pink, violet red colour in the ammonia phase indicated the presence of anthraquinones. Terpenoids were detected by the addition of 5 ml of the plant aqueous extract to 2 ml of chloroform then evaporation on a water bath before boiling with Conc-H₂SO₄. A grey colour formation indicated the presence of terpenoids. The Liebermann's test was applied to reveal the presence of glycosides by adding 2 ml of acetic acid to 2 ml of chloroform with a 5 ml plant crude aqueous extract solution. The mixture was then cooled and added to concentrated H₂SO₄. A green colour showed the presence of the aglycone, the steroidal part of glycosides.

5.5 | Green synthesis of phytochemical nanoparticles

5.5.1 | Taguchi orthogonal array (TOA)

Taguchi experimental design implemented on the Design-Expert version 12 was applied for designing and

optimization of the variables for green synthesis of *F. thonningii*-based silver nanoparticles. Based on preliminary screening experiments, the factors that would affect the rate and stability of nanoparticle formation included plant part, extraction solvent, extract volume and the stirring time.

These were all evaluated in single factor tests at different levels as indicated in Table 3. A L₉ (3⁴) Taguchi Orthogonal Array was then used to define the optimal conditions per the selected factors to produce *F. thonningii* silver-encapsulated nanoparticles and optimum temperature and stirring time for synthesis. Each of the nine experiments was performed in triplicate and the mean values recorded.

5.5.2 | Preparation of the *F. thonningii* nanoparticles

According to results of optimization, synthesis of *F. thonningii*-encapsulated AgNP's was done by mixing respective volume of the supernatant solution of the crude plant extract with 100 ml of the prepared 1 mM aqueous silver nitrate (AgNO₃) in a conical flask. This was then set on a magnetic stirrer to achieve encapsulation into nanoparticles by stirring for different time durations and with different extract volumes as per the optimization array. Samples from the nanoparticles synthesis media were harvested and scanned on the UV/Vis spectrophotometer for confirmation of NPs formation. The synthesised silver nanoparticles were then separated by micro-centrifugation at 10000 rpm and stored at 4°C awaiting characterisation.

5.6 | Characterization of the *F. thonningii* silver nanoparticles

5.6.1 | UV/Vis nanoparticle characterization

The carry 60 (Agilent) UV/Vis spectrometer was warmed for 30 min before setting the scan wavelength between 600 and 300 nm. The nanoparticle suspension was diluted appropriately and added in the cuvette. The cuvette was inserted in the sample compartment and the scan run was performed, read and recorded.

5.6.2 | ATR-FTIR nanoparticle elucidation

A neat sample was placed on the sample compartment of the ATR-FTIR instrument and scanned from 4000 to 400 cm⁻¹ wave number to identify fingerprints emanating from the respective samples. The spectra obtained were sent to the software library for peak comparison to identify the functional groups and interaction and orientations of the molecules present in the crude extract and synthesised AgNP's.

5.6.3 | Scanning Electron Microscopy (SEM)

Samples for SEM analysis were mounted on a stub and coated with a gold/palladium alloy in a sputter source. The sample was then firmly fixed onto the specimen mount with the entire surface to be observed exposed. The accelerating voltage was set at 10 kV and the working distance then adjusted to around 2 mm. The contrast and brightness were adjusted to optimal values so that the particles could be easily distinguished from the background. Further, the shape, morphology, and elemental mapping of *F. thoningii* AgNP's were studied.

5.6.4 | Dynamic Light Scattering and zeta potential analysis

Zetasizer Nano ZS, Malvern Panalytical, was used to determine the size distribution and zeta potential of prepared *F. thoningii* silver nanoparticles. The instrument was set to run at a rate of 60 times per scan with samples, each done in triplicate and the mean size distribution of nanoparticles adopted. The nanoparticle suspension was first diluted to a concentration of 100 µg/ml with homogenisation for 5 s to disaggregate the nanoparticles. Dynamic particle sizes were then determined by suspending 0.5 µl of the homogenized nanoparticle suspension in 1 ml of Millipore water in zetasizer cuvette followed by scanning of the nanoparticle suspension by the DLS analyser. Zeta potential of *F. thoningii* silver nanoparticles was measured by Zetasizer Nano ZS applying the electrophoretic light-scattering technology. Nanoparticle suspension at 1 mg/ml was prepared in Millipore water in a 900 µl zetasizer disposable cell. Similar to size, the suspension was assayed 60 times per scan also in triplicate and mean zeta potential of silver nanoparticles recorded.

5.7 | Antibacterial assays

The Agar well (Kirby-Bauer) method was adopted for evaluation and confirmation of antibacterial efficacy of the aqueous extracts and the *F. thoningii* silver nanoparticles. Test microorganisms were selected based on recommendation of National Committee for Clinical Laboratory Standards (NCCLS) as causative agents of secondary bacterial infections that affect the skin. The *S. aureus*, *S. pyogenes* and *E. coli* were selected as the test pathogens known for secondary skin infections. The strains (0.5 McF) were sub-cultured in 10 mL broth for 24 h in peptone water and seeded on Mueller-Hinton agar plates. A cork-borer was used to cut equal uniform wells of 6 mm on the plates and filled with 50 µL of test sample. The positive control was antimicrobial susceptibility disc flucloxacillin (1 µg) standard drug, while the negative control was deionised water (solvent of extraction). The *F. thoningii* crude extracts were screened for activity alongside the synthesised *F. thoningii* AgNPs. All these were incubated at 37°C for 24 h after which diameters of positive zones of inhibition are measured in millimetres and recorded. Minimum Inhibitory

Concentration (MIC) of the crude extracts and the *F. thoningii* encapsulated AgNP's sample with the highest antibacterial activity were then evaluated against the standard. The serial dilutions were screened for activity as previous and the zones of inhibition recorded accordingly.

5.8 | Statistical analysis

Analysis of Variance (ANOVA) was performed and results were tabulated accordingly for sum of squares, degree of freedom, and mean squares. The contributions of the various factors towards the phytochemical-based silver nanoparticle formation were also calculated by the formulae in Equation (I). All experiments were performed in triplicate and results reported as statistical means

$$\text{Percent Contribution (PC)} = \frac{\text{Sum of Squares (SS}_F\text{)}}{\text{Sum of Squares Total (SS}_{\text{Total}})} \times 100 \quad (\text{I})$$

ACKNOWLEDGEMENTS

The authors are thankful to the USIU-Africa for enabling the research by availing funds and laboratory facilities; and the School of Pharmacy & Health Sciences staff particularly Ms. Lucy Wambui of the USIU-Africa Herbarium for her assistance during sample collection. Much thanks to the Kenya Medical Research Institute for allowing access to their nanotechnology research laboratory equipment.

CONFLICT OF INTEREST STATEMENT

On behalf of all the authors, I confirm that there is no conflict of interest whatsoever as regards the research activities carried out and further publication of the results.

DATA AVAILABILITY STATEMENT

Data sharing is not applicable to this article as no datasets were generated or analysed during the current study.

FUNDING INFORMATION

The research was carried out with support of funds from the United States International University—Africa internal research grant.

PERMISSION TO REPRODUCE MATERIALS FROM OTHER SOURCES

None.

ORCID

Were L. L. Munyendo  <https://orcid.org/0000-0002-4261-8867>

REFERENCES

1. Betts, J.W., Hornsey, M.: La-Ragione RM. Novel antibacterials: alternatives to traditional antibiotics. *Adv. Microb. Physiol.* 73, 123–169 (2018)

2. Shaik, M.R., et al.: Plant-Extract-Assisted green synthesis of silver nanoparticles using *Origanum vulgare* L. Extract and their microbicidal activities. *Sustainability* 10(4), 913 (2018). <https://doi.org/10.3390/su10040913>
3. Umoren, S.A., Obot, I.B., Gasem, Z.M.: Green synthesis and characterization of silver nanoparticles using red apple (*Malus domestica*) fruit extract at room temperature. *J. Mater. Environ. Sci.* 5(3), 907–914 (2014)
4. Lakshmanan, G., et al.: Plant-mediated synthesis of silver nanoparticles using fruit extract of *Cleome viscosa* L.: assessment of their antibacterial and anticancer activity. *Karbala Intl. J. Mod. Sci.* 4(1), 61–68 (2018). <https://doi.org/10.1016/j.kijoms.2017.10.007>
5. Hosseinzadeh, N., et al.: Green synthesis of gold nanoparticles by using *Ferula persica* Willd. gum essential oil: production, characterization and in vitro anti-cancer effects. *J. Pharm. Pharmacol.* 72(8), 1013–1025 (2020). <https://doi.org/10.1111/jphp.13274>
6. Roy, A., et al.: Green synthesis of silver nanoparticles: biomolecule-nanoparticle organizations targeting antimicrobial activity. *RSC Adv.* 9(5), 2673–2702 (2019). <https://doi.org/10.1039/c8ra08982e>
7. Usman, A., Abdulrahman, F.I., Usman, A.: Qualitative phytochemical screening and in vitro antimicrobial effects of methanol stem bark extract of *Ficus thonningii* (Moraceae). *Afr. J. Tradit., Complementary Altern. Med.* 6(3), 289–295 (2009). <https://doi.org/10.4314/ajtcam.v6i3.57178>
8. Selvakumar, P., et al.: Synthesis of silver nanoparticles using *Acalypha indica* leaf extracts and its antibacterial activity against water borne pathogens. *Colloids Surf. B. Biointerfaces.* 76(1), 50–56 (2010). <https://doi.org/10.1016/j.colsurfb.2009.10.008>
9. MubarakAli, D., et al.: Plant extract mediated synthesis of silver and gold nanoparticles and its antibacterial activity against clinically isolated pathogens. *Colloids Surf. B. Biointerfaces.* 85(2), 360–365 (2011). <https://doi.org/10.1016/j.colsurfb.2011.03.009>
10. Dangarembizi, R., et al.: Phytochemistry, pharmacology and ethno-medicinal uses of *Ficus thonningii* (Blume Moraceae): a review. *Afr. J. Tradit., Complementary Altern. Med.* 10(2), 203–212 (2013). <https://doi.org/10.4314/ajtcam.v10i2.4>
11. Ndukwe, I.G., et al.: Phytochemical and antimicrobial screening of the crude petroleum spirit and methanol extracts of the stem bark, leaves and roots of *Ficus thonningii* (blume). *Afr. J. Biotechnol.* 6(23), 2645–2649 (2007). <https://doi.org/10.5897/ajb2007.000-2425>
12. Yuan, C.G., et al.: Biosynthesis of gold nanoparticles using *Capsicum annum* var. *grossum* pulp extract and its catalytic activity. *Phys. E Low-dimens. Syst. Nanostruct.* 85, 19–26 (2017). <https://doi.org/10.1016/j.physe.2016.08.010>
13. Selvaraj, R., et al.: Green synthesis of magnetic α -Fe₂O₃ nanospheres using *Bridelia retusa* leaf extract for Fenton-like degradation of crystal violet dye. *Appl. Nanosci.* 11(8), 2227–2234 (2021). <https://doi.org/10.1007/s13204-021-01952-y>
14. Vinayagam, R., et al.: Structural characterization of green synthesized magnetic mesoporous Fe₃O₄NPs@ME. *Mater. Chem. Phys.* 262, 124323 (2021). <https://doi.org/10.1016/j.matchemphys.2021.124323>
15. Prod, J.N., et al.: Phytochemical Screening and identification of some compounds from Mallow. *J. Nat. Prod. Plant Resour.* 2(4), 512–516 (2012)
16. Hamouda, R.A., et al.: Synthesis and biological characterization of silver nanoparticles derived from the cyanobacterium *Oscillatoria limnetica*. *Sci. Rep.* 9(1), 13071 (2019). <https://doi.org/10.1038/s41598-019-49444-y>
17. Kumar, C.: UV-VIS and Photoluminescence Spectroscopy for Nanomaterials Characterization. Springer Nature Switzerland AG (2013)
18. Mohammadlou, M., Maghsoudi, H., Jafarizadeh-Malmiri, H.: A review on green silver nanoparticles based on plants: synthesis, potential applications and eco-friendly approach. *Intl. Food Res. J.* 446–463 (2016)
19. Gogoi, N., et al.: Green synthesis and characterization of silver nanoparticles using alcoholic flower extract of *Nyctanthes arbortristis* and in vitro investigation of their antibacterial and cytotoxic activities. *Mater. Sci. Eng. C. Mater. Biol. Appl.* 46, 463–469 (2015). <https://doi.org/10.1016/j.msec.2014.10.069>
20. Rajeshkumar, S., Bharath, L.V.: Mechanism of plant-mediated synthesis of silver nanoparticles – a review on biomolecules involved, characterization and antibacterial activity. *Chem. Biol. Interact.* 273, 219–227 (2017). <https://doi.org/10.1016/j.cbi.2017.06.019>
21. Varghese, R., et al.: Silver nanoparticles synthesized using the seed extract of *Trigonella foenum-graecum* L. and their antimicrobial mechanism and anticancer properties. *Saudi J. Biol. Sci.* 26(1), 148–154 (2019). <https://doi.org/10.1016/j.sjbs.2017.07.001>
22. Amereh, F., et al.: Thyroid endocrine status and biochemical stress responses in adult male Wistar rats chronically exposed to pristine polystyrene nanoplastics. *Toxicol. Res.* 8(6), 953–963 (2019). <https://doi.org/10.1039/c9tx00147f>
23. Umoren, S.A., Obot, I.B., Gasem, Z.M.: Green synthesis and characterization of silver nanoparticles using red apple (*malus domestica*) fruit extract at room temperature. *J. Mater. Environ. Sci.* 5(3), 907–914 (2014)
24. Jacobs, C., Kayser, O., Müller, R.H.: Nanosuspensions as a new approach for the formulation for the poorly soluble drug tarazepide. *Int. J. Pharm.* 196(2), 161–164 (2000). [https://doi.org/10.1016/s0378-5173\(99\)00412-3](https://doi.org/10.1016/s0378-5173(99)00412-3)
25. Singh, P., et al.: Biological synthesis of nanoparticles from plants and microorganisms. *Trends Biotechnol.* 34(7), 588–599 (2016). <https://doi.org/10.1016/j.tibtech.2016.02.006>
26. Syafuddin, A., et al.: A review of silver nanoparticles: research trends, global consumption, synthesis, properties, and future challenges. *J. Chin. Chem. Soc.* 64(7), 732–756 (2017). <https://doi.org/10.1002/jccs.201700067>
27. Choi, K.C., et al.: Rapid green synthesis of silver nanoparticles from *Chrysanthemum indicum* L. and its antibacterial and cytotoxic effects: an in vitro study. *Int. J. Nanomed.* 9, 379–388 (2014). <https://doi.org/10.2147/ijn.s53546>
28. Zhang, X.F., et al.: Silver nanoparticles: synthesis, characterization, properties, applications, and therapeutic approaches. *Int. J. Mol. Sci.* 17(9), 1534 (2016). <https://doi.org/10.3390/ijms17091534>
29. Velusamy, P., et al.: Bio-inspired green nanoparticles: synthesis, mechanism, and antibacterial application. *Toxicol. Res.* 32(2), 95–102 (2016). <https://doi.org/10.5487/tr.2016.32.2.095>

How to cite this article: Ondigo, D.A., et al.: Enhancement of antibacterial activity through phyto-fabrication of silver nanoparticles with *Ficus thonningii* aqueous extracts. *IET Nanobiotechnol.* 16(7-8), 250–258 (2022). <https://doi.org/10.1049/nbt2.12093>